LA-UR-03-3084

Approved for public release; distribution is unlimited.

c.1

Title: RF COUPLER FOR HIGH-POWER CW FEL PHOTOINJECTOR

Author(s): Sergey S. Kurennoy, LANSCE-1
Lloyd M. Young, SNS-DO

42

Submitted to: 2003 Particle Accelerator Conference (PAC2003)
Portland, Oregon
May 12-16,2003

RF COUPLER FOR HIGH-POWER CW FEL PHOTOINJECTOR*

S.S. Kurennoy and L.M. Young, LANL, Los Alamos, NM 87545, USA

Abstract

A high-current emittance-compensated RF photo-injector is a key enabling technology for a high-power CW FEL. The design presently under way is a 100-mA, 2.5-cell π-mode, 700-MHz, normal conducting demonstration CW RF photoinjector. This photoinjector will be capable of accelerating 3 nC per bunch with an emittance at the wiggler less than 10 mm-mrad. The paper presents results for the RF coupling from ridged waveguides to the photoinjector RF cavity. The LEDA and SNS couplers inspired this "dog-bone" design. Electromagnetic modeling of the coupler-cavity system has been performed using both 2-D and 3-D frequency-domain calculations, and a novel time-domain approach with MicroWave Studio. These simulations were used to adjust the coupling coefficient and calculate the power-loss distribution on the coupling slot. The cooling of this slot is a rather challenging thermal management project.

INTRODUCTION

The project is underway to build a demonstration 700-MHz RF emittance-compensated CW photo-injector (PI) capable of accelerating 100 mA of the electron beam (3 nC per bunch at 33.3-MHz repetition rate) to about 5 MeV with the transverse emittance at the wiggler below 10 mm-mrad, see [1] and references therein. The PI consists of a 2.5-cell cavity with the accelerating gradient E_0=7 MV/m (the PI proper) that brings the electron beam energy to 2.7 MeV, followed by a 4-cell booster with E_0=4.5 MV/m, where the beam is accelerated to 5.5 MeV. This gradient choice is a trade-off between the beam-dynamics requirements and challenges of the cavity thermal management [2,1].

The injector is designed to be scalable to even higher beam currents, up to 1 A, and therefore, to higher beam power by increasing the bunch repetition rate. The high beam power plus a significant wall power loss in the normal-conducting PI cavity lead to serious challenges for cavity cooling. In addition to a large total RF power needed, there are regions of rather high loss power densities on the cavity walls. Therefore, we need to provide an effective RF power feeding to the PI cavity with the lowest possible increase of the surface power density. Here we present the design and electromagnetic modeling of the RF power couplers for the PI cavity.

RF COUPLER

The RF feeds are in the 3rd (the 2nd full) cell of the 2.5-cell PI cavity; see Fig. 1. Two symmetrically placed ridge-loaded tapered waveguides are connected to the cavity via "dog-bone" coupling irises – consisting of a long narrow slot with two circular holes at its ends – in a 0.5"-thick copper wall. This RF coupler design is based on the experience for the LEDA RFQ and SNS high-power RF couplers, e.g., see [3]. The required cavity-waveguide coupling is given by the coupling coefficient $\beta_c = (P_w + P_b)/P_w \approx 4/3$, where P_w=780 kW is the CW wall power loss [1], and P_b=270 kW is the beam power of a 100-mA beam at the 2.5-cell cavity exit. The coupling is adjusted by changing the radius of the holes at the ends of the coupler slot.

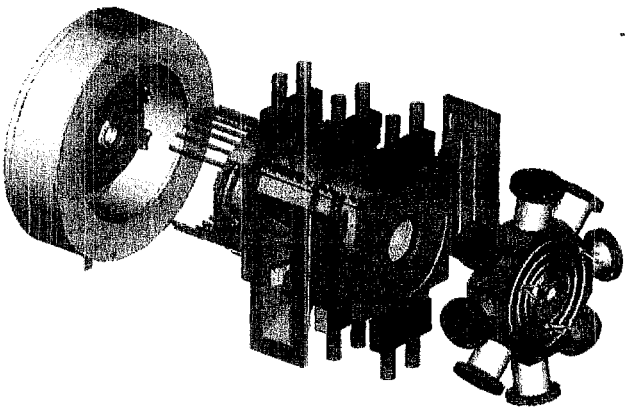

Figure 1: Schematic of 2.5-cell cavity with emittance-compensating magnets (left) and vacuum plenum (right).

Coupler Model

To simulate the waveguide-cavity system we use a simplified model shown in Fig. 2: a short pillbox cavity, which can be considered as a slice of the 3rd cell in the 2.5-cell PI cavity, with two attached short sections of the ridge-loaded waveguides. The picture shows only the internal (vacuum) part of the coupler model as used in simulations with the CST MicroWave Studio (MWS) [4].

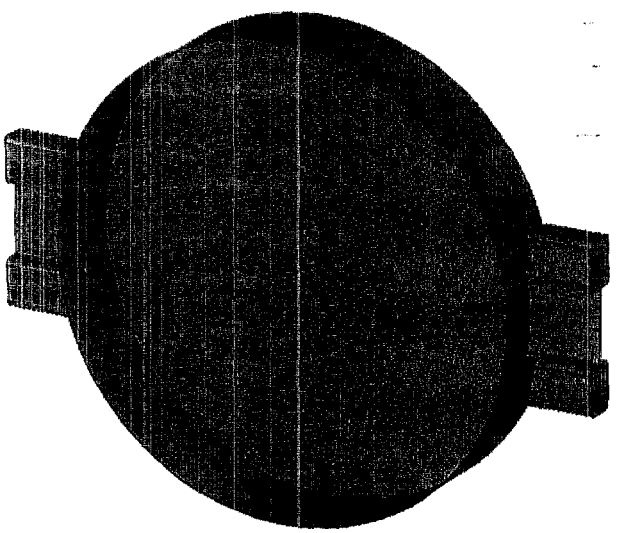

Figure 2: Model of pillbox cavity with two waveguides.

*Supported by the DoD High Energy Laser Joint Technology Office through a contract from NAVSEA.

The pillbox radius is slightly adjusted to provide the correct resonant frequency 700 MHz. Some model dimensions are listed in Tab. 1.

Table 1: Model dimensions

Parameter	**Value,** mm
Pill-box cavity radius	163.922
Pill-box length	60
Coupler slot length	50.8
Coupler slot width	1.434
Coupler end-hole radius	2.5

Obviously, for the pillbox cavity the waveguide-cavity coupling will be different than for the 2.5-cell PI cavity. It is related to the required β_c as

$$\beta_{pb} = \beta_c \frac{W_c}{W_{pb}} \frac{Q_{pb}}{Q_c}, \qquad (1)$$

where W_i, Q_i are the field energies and unloaded quality factors of the pill-box TM_{010} mode and the operating π-mode in the 2.5-cell cavity. We assume that W_{pb} is scaled such that the surface magnetic field far from the coupler iris in the transverse cross section at the coupler location is equal to one at the same location in the 3rd PI cell (14.8 kA/m) for the nominal PI gradient. From (1) the required waveguide-pillbox coupling is $\beta_{pb} \approx 6.1$.

Time-Domain Simulations with MWS

The waveguide-pillbox coupling is calculated directly with MWS time-domain simulations: the fields excited in the cavity with perfectly conducting walls decay due to radiation into the open waveguides. Due to the model symmetry, we restrict our simulations to 1/8 of the model, imposing the electric boundary conditions in *xy*-plane, and magnetic ones in *xz*- and *yz*-planes, cf. Fig. 2.

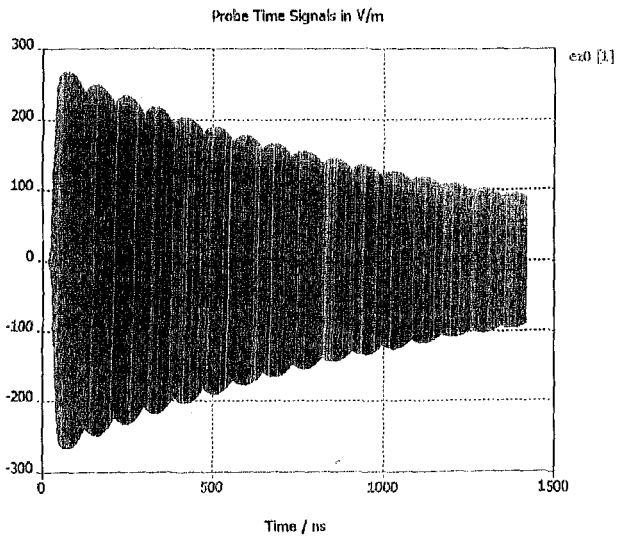

Figure 3: Electric field decay due to radiation into open waveguides as calculated by MWS.

The decay of the on-axis electric field excited in the cavity center by a short pulse from the waveguide is illustrated in Fig. 3. This particular computation on a mesh of about 50K points took 3.5 hours on a dual 1-GHz Pentium III Xeon PC. Inverting the calculated decay time constant gives us the external quality factor Q_e of the system, and then we find $\beta_{pb}=Q_{pb}/Q_e$ [4]. Starting from large slot-end holes (shorter computation times), we found that the required coupling $\beta_{pb}=6.1$ is achieved for a hole radius of 2.5 mm, cf. Tab. 1 and Fig. 3.

An exact resonance frequency of the pillbox-waveguide system is conveniently calculated with the auto regressive (AR) filter feature in MWS time-domain simulations. It allows one to analyze spectra of time signals that have not reached a steady state yet. With this technique we found the pillbox-waveguide resonance at f_r=699.575 MHz.

To calculate the power density distribution around the coupler during its nominal operation, we simulate the RF feeding of the model via the waveguides with a TE-mode at frequency f_r. The waveguide-mode fields are mostly concentrated in the narrow gap between the waveguide ridges, as shown in Fig. 4. The field scale corresponds to 1 W of the peak RF power fed through the waveguide.

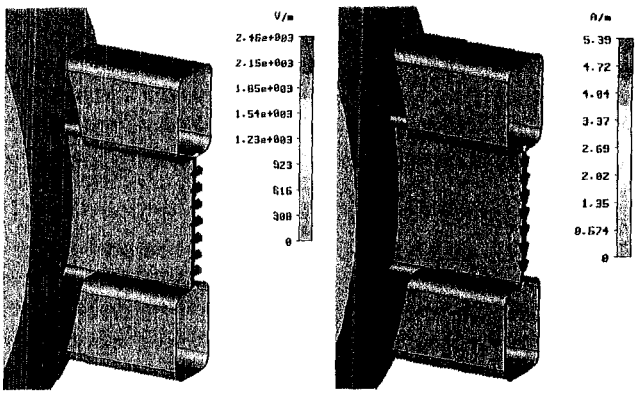

Figure 4: Electric (left) and magnetic (right) fields of the waveguide RF input mode.

The model symmetry means that the system is driven by two waveguides in phase. Calculated normalized time signals are plotted in Fig. 5. This plot, as well as one in Fig. 3, includes hundreds of oscillation periods; we see only signal envelopes. While the waveguide input remains constant, the output decreases reaching a point (t=956.6 ns) where it vanishes, and increases again after that. The output decrease is due to a destructive interference of two waves: one is reflected from the coupler aperture, and the other is radiated into the waveguides from inside the cavity. The reflected-wave amplitude remains constant when the input is constant, while the radiated-wave amplitude increases as the cavity field increases. These two waves are always in opposite phases [5]. As a result, at certain moment the two waves cancel each other, so that the reflected power vanishes at that particular moment. This situation corresponds to an exact match; therefore, the field snapshots at that moment give us field distributions for the matched case.

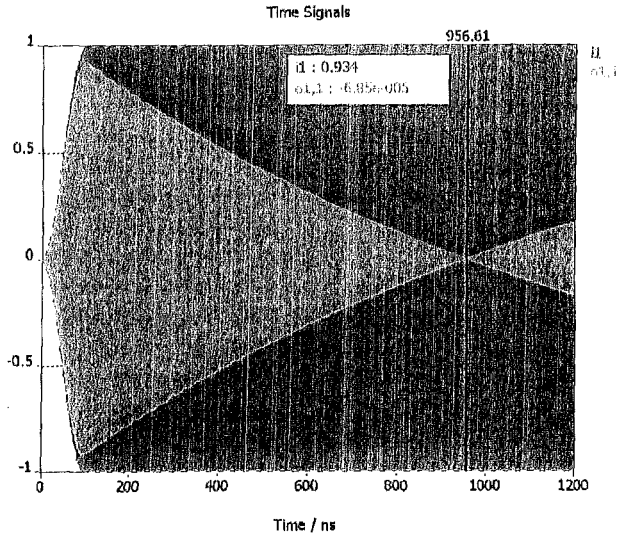

Figure 5: Input (red) and output (green) waveguide signals from MWS time-domain simulations.

The peak surface current magnitude at this moment is shown in Fig. 6. This picture was obtained using field monitors in MWS time-domain solver. The field scaling here is the same as for Fig. 4, i.e. 1-W peak RF power input into each of two waveguides.

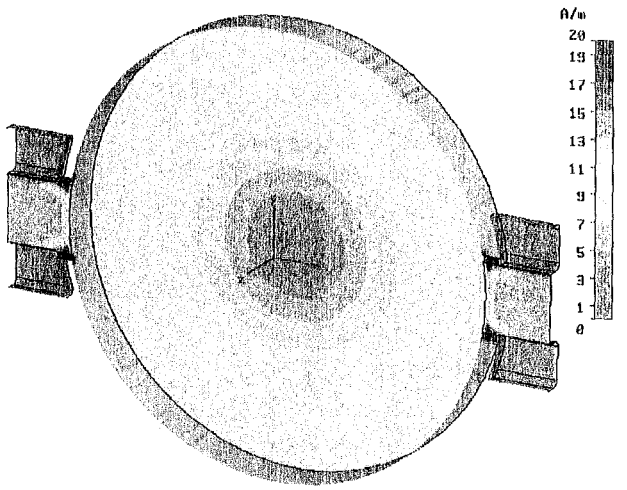

Figure 6: Peak surface current distribution at the moment of zero reflected power (view cut in *xy*-plane).

One can see that the surface power densities are the highest near the ends of the slot aperture. Comparing the magnetic field on the cylindrical wall far from the coupler with one at the coupler location in the 2.5-cell cavity for the nominal field gradient, we find a field-scaling factor. Some results for rescaled fields and power values are presented in Tab. 2. The rescaled averaged RF power transferred through each of the two waveguides is about 525 kW, as should follow from the energy balance for the matched waveguide-cavity coupling.

Table 2: Fields and power in 2.5-cell cavity with couplers

Parameter	Value
Surface magnetic field on the wall in the 3rd cell far from the coupler*	14.8 kA/m
Power density on the smooth wall in 3rd cell far from the coupler	76 W/cm^2
Maximal surface magnetic field near the coupler slot ends	24.4 kA/m
Maximal power density near the coupler slot ends	205 W/cm^2
Maximal power density elsewhere in 2.5-cell PI cavity w/o RF couplers**	107 W/cm^2

* In the transverse cross section at the coupler location.
** On the upstream wall of the 1st half-cell [1].

CONCLUSIONS

Electromagnetic modeling of the coupler-cavity system has been performed using 2-D (Superfish) and 3-D (MWS) frequency-domain calculations, plus a novel time-domain approach using the MicroWave Studio. These simulations were applied to adjust the coupling coefficient and calculate the power-loss distribution on the coupling slot.

The cooling of the regions around the coupling irises is a challenging thermal management issue due to the surface power density exceeding 200 W/cm^2 at some points. However, since the hot spots are localized in small regions around the slot ends, they can be cooled effectively with cooling channels placed properly around the slots in the thick cavity wall.

The authors would like to acknowledge useful discussions with F. Krawczyk, D. Schrage, and R. Wood (LANL), as well as with J. Rathke and T. Schultheiss of Advanced Energy Systems.

REFERENCES

[1] S.S. Kurennoy, et al. "Photoinjector RF Cavity Design For High Power CW FEL", these proceedings.

[2] S.S. Kurennoy, et al. "CW RF Cavity Design for High-Average-Current Photoinjector for High Power FEL", FEL'02, Argonne, IL, Sep. 2002.

[3] L.M. Young, et al. "High Power RF Conditioning of the LEDA RFQ", Proceed. 1999 PAC, NY, p. 881.

[4] MicroWave Studio v. 4.2, CST GmbH (Darmstadt, Germany), 2003. www.cst.de.

[5] T.P. Wangler, *RF Linear Accelerators*, Wiley, NY, 1998.